53rd AIAA/SAE/ASEE Joint Propulsion Conference, AIAA Propulsion and Energy Forum,
(AIAA 2017-5055) DOI: 10.2514/6.2017-5055

Performance Assessment of a Boundary Layer Ingesting Distributed Propulsion System at Off-Design

C. Goldberg*, D. Nalianda† P. Laskaridis‡ and P. Pilidis§
Cranfield University, Bedfordshire, MK43 0AL, United Kingdom

Abstract

As research on boundary layer ingesting aircraft concepts progresses, it becomes important to develop methods that may be used to model such propulsion systems not only at design point, but also over the full flight envelope. This research presents a methodology and framework for simulating the performance of boundary layer ingesting propulsion systems at off-design conditions. The method is intended for use as a preliminary design tool that may be used to explore the design space and identify design challenges or potential optimum configurations. The method presented in this research enables the rapid analysis of novel BLI configurations at a preliminary design stage.

The method was applied to a case study of NASA's N3-X aircraft, a blended wing body concept with a distributed propulsor array ingesting the airframe boundary layer. The performance of two propulsor in the array was compare, one at the airframe centreline and one at the extreme edge of the array. Due to difference in flow conditions, the centreline propulsor was shown to be more efficient at off-design than the end propulsor. However, this difference in efficiency disappeared at sea level static where the boundary layer thickness is negligible and mass flow ratio is high. Difference in thrust produce by the two propulsors was instead due their different sizes.

Performance of the propulsor array as a whole was also presented both independently and including a link to a pair of turbogenerators to provide power. At off design, it was found that there was a discrepancy between the maximum power available from the turbogenerators at off-design operating points and that demanded by the propulsor array operating at 100% fan rotational speed. This discrepancy means that the propulsor array's performance is limited by the turbogenerators at off-design, particularly for low speed, low altitude operation.

Nomenclature

Acronyms

ADP	=	Aerodynamic design point
AR	=	Aspect ratio
BLI	=	Boundary layer ingestion
MAG	=	Mass flow group
MFR	=	Mass flow ratio
NDMF	=	Non-dimensional mass flow
NPF	=	Net propulsive force
PSC	=	Power saving coefficient
RTO	=	Rolling take-off
SFC	=	Specific fuel consumption
SPC	=	Specific power consumption
TET	=	Turbine entry temperature

Symbols

A	=	Area
D	=	Drag
F_{G9}	=	Gross thrust

*Research Assistant, Hybrid Electric Propulsion Group, Propulsion Engineering Centre, Cranfield University. Student Member
†Lecturer, Hybrid Electric Propulsion Group, Propulsion Engineering Centre, Cranfield University.
‡Senior Lecturer, Hybrid Electric Propulsion Group, Propulsion Engineering Centre, Cranfield University.
§Head of Centre, Propulsion Engineering Centre, Cranfield University.

F_{Gi}	=	Momentum drag
h	=	Height of streamtube
$\dot{m}$	=	Mass flow rate
P	=	Pressure
S_{wet}	=	Wetted surface area
T	=	Temperature
u	=	Velocity
w	=	Width
y	=	Distance above fuselage surface
δ	=	Boundary layer thickness
η	=	Efficiency
ρ	=	Density
τ_w	=	Skin friction

1 Introduction

Aircraft concepts are being developed that make use of novel configurations to achieve improvements in efficiency through performance benefits to the airframe and propulsion system. Boundary layer ingestion (BLI) is one such technology that has been implemented in a number of conceptual designs. In an aircraft, the boundary layer contributes to drag and results in a momentum deficit, or wake, and is therefore detrimental to performance. The boundary layer can be similarly detrimental to the propulsion system, as a turbulent boundary layer gives rise to non-uniformities in the flow which negatively impact performance. Conventional propulsion system design therefore typically seeks to avoid ingesting any boundary layer flow. This is generally achieved by methods such as bleeding/diverting the boundary layer away from an inlet or with podded engines well outside the airframe's boundary layer. However, boundary layer ingestion provides a way in which the boundary layer may be used to improve the overall efficiency of the aircraft and reduce fuel consumption. Rather than ingesting only free-stream flow, a BLI propulsor ingests some or all of the boundary layer. The resulting lower average velocity of the boundary layer flow reduces the momentum drag at the inlet of a propulsion system. The same thrust may therefore be produced using less power than an equivalent propulsion system in free-stream flow [1]. Boundary layer or wake ingestion as a concept is already implemented in marine propulsion, and research suggests that it can provide similar benefits to efficiency in aviation applications [2]. Research has shown that fuel savings in the region of 5-10% can be achieved by using boundary layer ingestion as opposed to a conventional free-stream propulsion system [2–4].

Simulating the performance of a boundary layer ingesting propulsion system presents a number of challenges. In a conventionally podded engine configuration, the airframe and engine may easily be differentiated. This supports conventional thrust-drag bookkeeping, where the forces resulting from each system may be relatively easily identified. However, in a BLI system, the propulsion system is closely integrated with the airframe. The propulsion system influences airflow over the airframe and vice versa, therefore complicating conventional propulsion system bookkeeping. To circumvent the difficulty of thrust-drag bookkeeping in an integrated BLI system, the power balance method developed by Drela assesses the aircraft system as a whole [5]. A similar method was presented by Arntz et al that uses an exergy analysis of the aircraft and propulsion system [6]. Alternative methods make use of a more conventional force control volume for the propulsion system alone [1, 7, 8]. In these cases, an appropriate thrust-drag split between the airframe and propulsion system is required to adequately represent the propulsion system and its performance. Methods that simulate the aircraft and engine as a combined system avoid the challenges of separately simulating the two components of an integrated system. However, such methods are reliant on a more detailed knowledge of the configuration, which is less suited to the conceptualisation of a propulsion system configuration. In addition, conventional point mass based aircraft performance models are typically reliant on the ability to separate the thrust and drag of the aircraft and propulsion system. Methods based on more conventional force control volumes are therefore useful at the early stages of design, particularly as aircraft and propulsion system design will typically be conducted by different design groups.

As aircraft concepts advance through design stages, research is required to predict their mission performance. As a part of this development, simulations of the propulsion system are required over the full flight envelope. Typically, research on performance of BLI systems focuses on proving and identifying the benefits of a BLI system and hence focuses on design point sizing and performance. However, as research progresses on BLI systems, a more complete assessment of performance at a range of operating points is vital to fully understand performance. There is therefore a gap in research on tools for off-design simulation to predict performance over the full course of a mission and over the operating envelope. Such tools enable the full

design space to be explored in order to inform decisions during the conceptualisation and preliminary design phase of development.

This research presents the extension of a previously developed design-point simulation tool [8] for use in off-design simulations. This model was subsequently applied to a case study of NASA's N3-X aircraft [9] and will expand on previous research by the authors in simulating the aircraft's propulsion system.

2 Thrust and Drag Accounting

The forces produced by an aircraft in flight can be split to belong to either a propulsion system or an airframe force accounting system in support of conventional descriptions of aircraft performance simulation methods [10]. Airframe drag may then be used to determine propulsion system requirements, such as the requirement that in steady level flight, the net thrust produced by a propulsion system should counter drag. For aircraft with more integrated architectures, it becomes more difficult to differentiate between the airframe and the propulsion system forces [3]. Nevertheless, it is useful to have a way of differentiating the two for ease of design and simulation. Typically, thrust is defined as a 'standard net thrust' term, the difference between the gross thrust at the nozzle exit and the gross thrust far upstream. However, a boundary layer ingesting propulsion system is an integrated system with performance that is closely linked to the airframe. In an integrated or installed system, additional terms may also be assigned to the propulsion side of thrust-drag bookkeeping. Performance may instead be represented by a Net Propulsive Force (NPF) term, which includes the force terms associated with engine installation.

In a BLI system, flow entering the inlet has passed over the surface of the aircraft fuselage. It could therefore be argued that the entire fuselage section prior to the inlet is a part of the propulsion system control volume. However, this complicates performance calculations for both the airframe and propulsion system as a portion of the airframe's drag will be influenced by the propulsion system. A control volume encompassing the entire upstream flow would result in an engine performance calculation that required aircraft performance and operating data at every operating point (e.g. aircraft angle of attack). In contrast, for a control volume covering only the propulsion system, the aircraft drag calculations would be linked to engine performance. Airframe drag would vary as a result of the engine's performance, as engine suction would accelerate or decelerate flow into the inlet. Skin friction drag ahead of the inlet would therefore be linked to the propulsion system. Instead, a suitable interface point, i, (Figure 1) should be chosen which indicates the region where engine thrust and drag is no longer a function of the aircraft condition, and vice versa. This is estimated to lie approximately two inlet heights ahead of the highlight [11, 12].

As with a conventional propulsion system, the net thrust should counterbalance the aircraft drag in steady level flight. However, the control volume is defined to begin slightly ahead of the inlet at the interface point. Therefore, the net propulsive force may be defined as follows:

$$\mathrm{NPF} = F_{G9} - F_{Gi} - \tau_w S_{\mathrm{wet}} - D_{\mathrm{nacelle}} = D_{\mathrm{aircraft,clean}} \tag{1}$$

$$F_G = \dot{m}u + A(p - p_0) \tag{2}$$

Where F_{G9} is the gross thrust, and F_{Gi} is the momentum drag, $\tau_w S_{\mathrm{wet}}$ is the skin friction of the surface from the interface point to the inlet, D_{nacelle} is the nacelle's drag, and $D_{\mathrm{aircraft,clean}}$ is the drag of the aircraft without the propulsion system. The difference between F_{G9} and F_{Gi} is analogous to the conventional net thrust term used in propulsion. Following this net propulsive force formulation, performance of a BLI propulsion system may be estimated in a similar manner to that of a conventional propulsion system with one dimensional gas dynamics methods. However, the simulation process now begins with an estimation of the flow characteristics at the interface point, i. In a conventional propulsion system, these flow characteristics are equal to those of the free-stream flow and hence F_{Gi} is equal to F_{G0}. However, in a BLI system, the inlet flow characteristics are a function of the boundary layer and will depend on both the boundary layer flow characteristics and the percentage of boundary layer or free-stream air ingested (ratio h/δ). This formulation also supports the use of conventional aircraft performance methods by maintaining a separation between the airframe and propulsion system for the purposes of simulation.

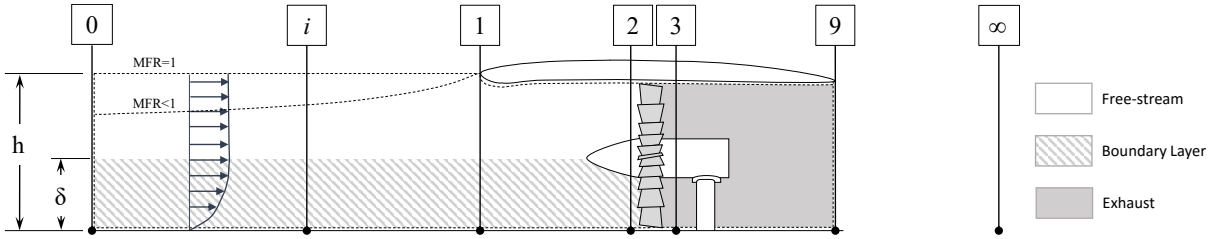

Figure 1: Propulsion system control volume and station definition.

3 Methodology

3.1 Inlet Flow Characteristics

To assess the performance of a BLI propulsion system using the net thrust formulation in Equation 1, three key parameters are required; mass flow, velocity, and pressure (Equation 2). For a BLI system, these parameters depend on where in the boundary layer these flow characteristics are measured. However, this may be simplified by assuming that the inlet flow characteristics are the average of the flow characteristics of the inlet streamtube. Inlet flow characteristics for a BLI propulsion system are therefore dependent on the flow being ingested. Three options may be considered for a BLI system:

1. Ingest only the boundary layer ($h/\delta = 1$).
2. Ingest free-stream and the boundary layer ($h/\delta > 1$).
3. Ingest a portion of the boundary layer ($h/\delta < 1$).

Flow characteristics outside the boundary such as velocity and pressure and constant and equal to the free-stream values. Flow characteristics in the boundary layer itself can be estimated using equations derived from the Navier-Stokes equations for viscous flow. These may be reduced to a more easily solvable form by applying appropriate limits to the integrals and through the use of velocity profile approximations [13]. One such approximation is the $1/n^{\text{th}}$ power law relationship, where $n = 7$ is a value often used to represent a fully developed boundary layer [14]. Whilst alternative approximations are available, the power law provides a useful relationship for preliminary simulations. Similarly, a number of approximations are available for predicting the boundary layer thickness, depending on the body configuration and whether flow is laminar or turbulent. One such boundary layer thickness estimation is a simple turbulent flat plate approximation of the boundary layer[15]:

$$\delta = \frac{0.37x}{Re_x^{1/5}} \tag{3}$$

A number of additional dimensions that define the boundary layer are available: the displacement thickness (δ^*), momentum thickness (θ), and energy thickness (θ^*) [16]:

$$\frac{\delta^*}{\delta} = \int_0^\infty \left[1 - \frac{\rho_y}{\rho_0}\frac{u_y}{u_0}\right] \mathrm{d}y \tag{4}$$

$$\frac{\theta}{\delta} = \int_0^\infty \frac{\rho_y}{\rho_0}\frac{u_y}{u_0}\left[1 - \frac{u_y}{u_0}\right] \mathrm{d}y \tag{5}$$

$$\frac{\theta^*}{\delta} = \int_0^\infty \frac{\rho_y}{\rho_0}\frac{u_y}{u_0}\left[1 - \left(\frac{u_y}{u_0}\right)^2\right] \mathrm{d}y \tag{6}$$

Each boundary layer thickness term represents the distance by which the surface would have to be displaced in an inviscid flow in order to result in the same mass flow, momentum or kinetic energy as the viscous flow.

The three key flow characteristics for F_G can be estimated in a similar manner by integrating over the height of the inlet streamtube. The values may be determined non-dimensionally relative to free-stream flow characteristics:

$$\frac{\dot{m}_\mathrm{i}}{\rho_0 u_{0i} \delta w} = \int_0^{h/\delta} \frac{\rho_y}{\rho_0}\frac{u_y}{u_{0i}} \mathrm{d}\left(y/\delta\right) \tag{7}$$

$$\frac{\overline{P}_i}{P_0} = \frac{1}{\mathrm{MAG}} \int_0^{h/\delta} \frac{P_y}{P_0}\frac{\rho_y}{\rho_0}\frac{u_y}{u_{0i}} \mathrm{d}\left(y/\delta\right) \tag{8}$$

$$\frac{\overline{u}_i}{u_0} = \frac{1}{\mathrm{MAG}} \int_0^{h/\delta} \frac{\rho_y}{\rho_0} \left(\frac{u_y}{u_{0i}}\right)^2 \mathrm{d}\left(y/\delta\right) \tag{9}$$

Where MAG is the mass flow in the boundary layer non-dimensionalised by the mass flow of free-stream flow through the same cross-sectional area [8]:

$$\mathrm{MAG} = \frac{\dot{m}_{\mathrm{BL}}}{\rho_0 u_{0i} \delta w} = \int_0^1 \frac{\rho_y}{\rho_0} \frac{u_y}{u_0} \mathrm{d}\left(y/\delta\right) = 1 - \frac{\delta^*}{\delta} \tag{10}$$

Both the average total pressure of the inlet streamtube, $\overline{P}_i$, and the average velocity of the inlet streamtube, $\overline{u}_i$, are mass-flow averaged parameters. When the inlet height, h, is equal to or greater than the boundary layer thickness, δ, the integrals may be simplified to functions of the boundary layer flow characteristics and the ratio h/δ:

$$\frac{\dot{m}_{\mathrm{i}}}{\rho_0 u_{0i} \delta w} = \left(\frac{h}{\delta} - 1\right) + \mathrm{MAG} \qquad h \geq \delta \tag{11}$$

$$\frac{\overline{P}_i}{P_0} = \frac{(\frac{h}{\delta} - 1) + \mathrm{MAG}(\frac{\overline{P}_{BL}}{P_0})}{(\frac{h}{\delta} - 1) + \mathrm{MAG}} \qquad h \geq \delta \tag{12}$$

$$\frac{\overline{u}_i}{u_{0i}} = \frac{(\frac{h}{\delta} - 1) + \mathrm{MAG}(\frac{\overline{u}_{BL}}{u_{0i}})}{(\frac{h}{\delta} - 1) + \mathrm{MAG}} \qquad h \geq \delta \tag{13}$$

In this form, inlet flow characteristics are determined non-dimensionally and independently from the propulsion system size. This simplifies the sizing process of a propulsor, as boundary layer flow characteristics are constant for a fixed flight condition. The three relevant boundary layer flow characteristic terms MAG, $\overline{P}_{BL}/P_0$ and $\overline{u}_{BL}/u_{0i}$ may be calculated from Equations 7–9, with limits from 0 to 1. Hence, MAG, $\overline{u}_{BL}/u_{0i}$ and $\overline{P}_{BL}/P_0$ are independent from the propulsion system's size and performance, whilst only h/δ is linked to the propulsion system size and performance. Inlet flow characteristics may then be simply determined as a function of h. It should be highlighted that where h is less than δ, Equations 11–13 cannot be used. Instead, the three ratios must be calculated using Equations 7–9, with limits from 0 to h/δ , where h/δ is less than 1. Once the average inlet flow characteristics have been determined, conventional 1D gas dynamics methods may be used to estimate the performance of the propulsors.

3.2 Design Point Performance

Whilst boundary layer flow characteristics are fixed for a set flight condition, the characteristics will be dependent on the propulsor's location. A propulsor located at the trailing edge of a fuselage will ingest a significantly larger boundary layer than a propulsor located near the leading edge. The local velocity of the free-stream flow entering a propulsor may also depend on the aircraft configuration due to the velocity profile over the fuselage. For blended wing body type configurations, the aerofoil cross-section leads to a flow acceleration and subsequent deceleration from the leading to trailing edges. Non-lifting fuselages such as the fuselage of a tube-and-wing will experience a deceleration of flow due to the skin friction (leading to the aircraft wake). Propulsion system performance therefore cannot be determined entirely independently from the aircraft and will rely on an estimate of the aircraft configuration. Location and configuration factors will play a significant effect on the performance of a propulsor, and means each propulsor should be individually sized for the best performance given its location [17].

The first step in the process establishes the local flow characteristics (including Reynolds number, boundary layer thickness and local free-stream velocity at the edge of the boundary layer). Subsequently, the boundary layer flow characteristics and inlet flow characteristics may be determined. Finally, the inlet flow characteristics are used to calculate the performance of the propulsor using conventional one dimensional gas dynamics (Figure 2). Previous research by the authors presented simulations of a case study configuration using the design point method [8].

Similar to a conventional propulsion system, the size of a propulsor is determined by the propulsive force required. However, in the case of a BLI system, changes to the propulsor and inlet dimensions will influence the averaged flow characteristics at the interface point. Estimation of the size of a BLI propulsor using the method used in this research therefore necessitates a procedure that solves for a propulsor size which produces the required net propulsive force. In order to simplify the analysis, it is assumed that the thickness of the boundary layer does not vary significantly over the width of the inlet streamtube. However, this assumption may break down depending on the configuration of the aircraft and the width of the propulsor.

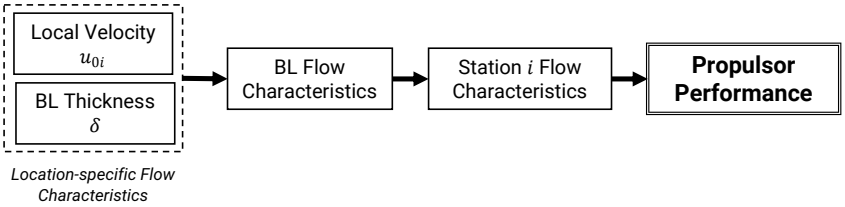

Figure 2: BLI propulsor simulation method at design point

3.3 Off-design Extension

The design point process can be used to determine the requisite size of a propulsion system for a defined design point. At off-design, the performance propulsor depends on the running line of its components. A key aspect of this is the mass flow demand of the components, which may be presented as a non-dimensional mass flow (NDMF) that allows the mass flow to be presented independently from flight conditions:

$$\mathrm{NDMF} = \frac{\dot{m}\sqrt{T}}{P} \tag{14}$$

For a fan/compressor, the running line provides a relationship between the mass flow through the component, its pressure ratio, and its rotational speed (Figure 3). The mass flow demanded by the operating point of each component must be matched to the operating point of other components within the propulsion system. In a conventional propulsion system, an iterative process can be used to determine the operating point where mass flow demand for each component is matched, based on the propulsion system's design size, power setting and flight conditions. Subsequently, the off-design operating point of each component of the system may be used to determine its performance. The size of the inlet stream varies depending on the resulting mass flow demand of the system, with a high mass flow demand resulting in a larger cross-sectional area for the incoming streamtube of air. This can be linked to the mass flow ratio (MFR) term; the ratio of inlet area to the streamtube area.

For a propulsion system operating in free-stream flow, the size of the streamtube will influence its mass flow alone as total pressure and velocity of the incoming air are only functions of the flight velocity and altitude. However, for a BLI system, the size of the streamtube will have a noticeable effect on the incoming flow characteristics in addition to the mass flow. For a fixed flight condition, the boundary layer thickness at station i and the boundary layer flow characteristics are constant. However, h/δ will be a function of the mass flow demand. Therefore, following Equations 11–13, the inlet flow characteristics will vary as a function of the mass flow demand, mass flow ratio, and hence the propulsor's operating point. An engine operating with a high mass flow ratio may ingest predominantly free-stream air, with a very high ratio of h/δ. In contrast, a propulsor operating with a low mass flow ratio may ingest predominantly boundary layer and potentially less than the entire boundary layer. The boundary layer thickness is also a function of the flight conditions. For example, a slow-moving or static aircraft will have a negligible boundary layer thickness. At sea-level static conditions, a negligible boundary layer and high mass flow ratio (high h/δ) means that inlet flow characteristics tend towards their free-stream values, and a propulsor may therefore perform very similarly to a conventional free-stream propulsor. The combination of these factors means that flow characteristics and hence non-dimensional mass flow are a function of the size of the inlet stream.

Given this relationship between flow characteristics and the size of the inlet stream, a mass-flow matching procedure is required to match the upstream mass flow and streamtube size to the mass flow demanded by the propulsor. Note that it has been assumed that the flow is isentropic and that there is therefore no loss in total temperature. Matching for the mass flow of a fan only:

1. Mass flow at interface point (Equation 11)
2. Total pressure at fan face (including the total pressure deficit of the boundary layer, Equation 12)
3. Mass flow at fan face (Equation 14)
4. Iterate stream height h to match mass flows

For a complete propulsion system, the operating point and mass flow demand of each component will lead to the mass flow demand required to match the streamtube mass flow. This mass flow matching procedure should be included within the overall process to determine the engine's operating point. As the non-dimensional mass flow is a function of the engine's operating point, multiple iterative loops may be required to obtain a matched operating point. Once the engine's operating point has been determined and the mass flow matching procedure is complete, the performance of the propulsion system may be estimated by following conventional 1D gas dynamics methods, as with the design point method (Figure 4).

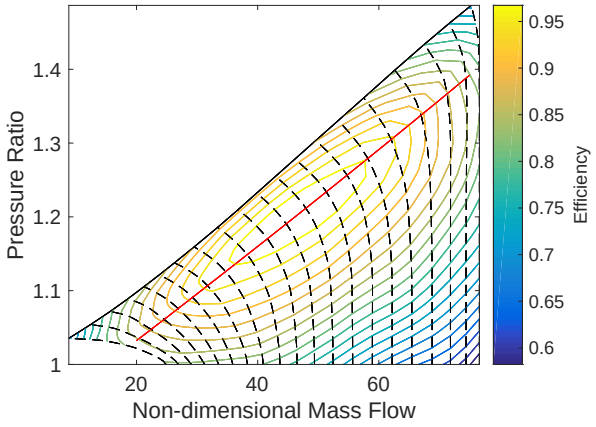

Figure 3: Generic scaled fan map with peak efficiency running line

The present research focuses on a propulsor consisting of an intake, fan, and a variable area nozzle. Where the nozzle has a variable area the only matching required is between the streamtube and fan mass flows. It may therefore be assumed that NDMF is constant for a fixed engine rotational speed. The mass flow matching for this case makes use of the following relationships:

$$\dot{m}_{\mathrm{i}} = \left[\left(\frac{h}{\delta} - 1\right) + \mathrm{MAG}\right] \times \rho_0 u_{0i} \delta w \tag{15}$$

$$\dot{m}_2 = \frac{\mathrm{NDMF} \times P_2}{\sqrt{T_2}} \tag{16}$$

$$P_2 = p \frac{P_0}{p} \frac{\overline{P}_i}{P_0} \eta_1 \tag{17}$$

Where η_1 is the total pressure loss through the inlet and P_2 is a function of h/δ through $\overline{P}_i$ (Equation 12). Depending on the configuration, an additional term may be required to determine the total pressure loss due to separation of the incoming flow at the lip or of the boundary layer. The goal of the matching procedure is to obtain the value of h/δ where the following equality is true:

$$\dot{m}_2 = \dot{m}_{\mathrm{i}} \tag{18}$$

A similar equality will apply to propulsion systems consisting of any number of components. This value of h/δ may be used to calculate the average velocity at the inlet (Equation 13), and subsequently, the propulsor's performance.

A number of additional general assumptions were also applied for simulating a BLI propulsion system's performance at off-design:

- Flow at interface point is independent of propulsor demand
- Constant ratio of free stream to boundary layer air from the interface point onwards (h/δ)
- Streamtube flow characteristics are averaged from the interface point onwards
- Square streamtube cross-section of constant width

Given the steamtube cross-section assumption, the mass flow ratio of the propulsor may be defined as follows:

$$\mathrm{MFR} = \frac{A_i}{A_H} = \frac{h}{h_H} \tag{19}$$

3.4 Inlet Total Pressure Loss

An ingested turbulent boundary layer can give rise to total pressure and swirl non-uniformities which can have a negative impact on the performance of an engine. The distortion in the inlet can lead to higher total pressure loss in the inlet than for an engine that ingests laminar free-stream flow. In some cases, the adverse pressure gradient through an intake may lead to boundary layer separation. Boundary layer ingesting systems are often

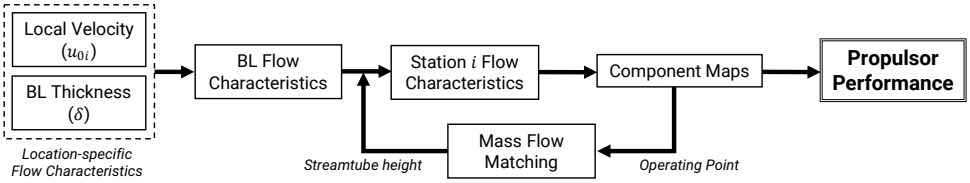

Figure 4: BLI propulsor simulation method at off-design

paired with s-duct intakes, to allow for greater integration in the airframe. This configuration is particular at risk of separation, and research has been conducted to determine how best to limit inlet distortion [18, 19]

Seddon developed a method to predict the total pressure loss in an inlet ingesting boundary layer air [20]. The method estimates the total pressure loss as a function of the mass flow ratio, the inlet aspect ratio, the flight speed, and boundary layer capture ratio. This method was used to provide an estimate of the total pressure loss in the inlet resulting from the boundary layer for any flight condition.

Previous research has shown that the efficiency of BLI propulsors is sensitive to the total pressure loss in the inlet [8]. This is particularly apparent for low pressure ratio propulsors, as the total pressure loss lowers the effective pressure ratio. The propulsor must therefore ingest more mass flow to produce the required thrust, and will therefore be larger than a system with a lower total pressure loss in the inlet. A larger system may also be required to ingest more free-stream mass flow, hence tending inlet flow characteristics to free-stream and reducing the benefits gained by ingesting the boundary layer.

3.5 Fan Compression Efficiency

The non-uniform flow of the boundary layer will negatively impact the efficiency of components ingesting the boundary layer. Depending on the type of distortion, the non-uniform flow may lead to surge in certain sections of the propulsor, requiring a fan with an appropriate surge margin [1]. The non-uniform flow will also impact the mechanical integrity of the fan blades [21].

The developed method does not directly represent the loss of efficiency result. Alternative methods such as the parallel compressor method have been used to estimate the average efficiency of compression [22]. Previous research showed that the efficiency of a BLI propulsor is less sensitive to fan efficiency than to the total pressure loss in the inlet (assuming surge is avoided). A loss in efficiency leads primarily to a step increase in power consumption, with little change in the thrust produced [8].

3.6 Representing Efficiency

The efficiency of a boundary layer ingesting propulsion system is often presented in terms of a Power Saving Coefficient (PSC) [1, 22, 23]. This metric was first proposed by Smith and compares the power consumption of a BLI propulsor against an equivalent propulsor producing the same thrust using free-stream air [2]. As the primary goal of a BLI propulsion system is to increase efficiency, the power saving coefficient enables insight on whether BLI is beneficial for a configuration.

Another commonly used metric is propulsive efficiency. Propulsive efficiency for a BLI system is defined in a similar manner to a conventional propulsion system [24]:

$$\eta_{\text{prop}} = \frac{2u_0}{\overline{u}_i + u_j} \tag{20}$$

Unlike a conventional propulsion system, the velocity of air ingested by a BLI system, $\overline{u}_i$ is not equal to the free-stream velocity u_0. The propulsive efficiency tends to the conventional definition as the ingested velocity tends to the free-stream velocity. As a result of this definition, the propulsive efficiency of a BLI system can be greater than 100% and will typically be higher than that of a conventional propulsion system. The propulsive efficiency metric does not completely capture any losses in efficiency that result from boundary layer-related distortion in a propulsion system. A system could therefore have a high propulsive efficiency but consume more power/fuel than a system operating in free-stream flow.

The power saving coefficient is useful as a comparative term against a conventional system, however, it is also useful to have an efficiency metric that may be used without defining a system against which BLI must be compared. A metric analogous to the thrust specific fuel consumption (SFC) will be used here; a 'thrust specific power consumption' (SPC):

$$\text{SPC} = \frac{\text{Power}}{\text{NPF}} \tag{21}$$

This metric presents the power required by a propulsor per unit propulsive force produced. Whilst specific fuel consumption can be used for fuel-burning systems, power is the more useful term for electrically driven systems. As with SFC, a lower SPC implies a more efficient system that uses less power.

It is also possible to make use of the h/δ ratio to predict efficiency. A higher proportion of ingested free-stream air (high h/δ) implies a system with inlet flow characteristics tending to free-stream, and may therefore be less efficient than a system ingesting only the boundary layer.

4 Case Study Definition

The present research focuses on a case-study of the NASA N3-X conceptual aircraft, developed by Felder et al [4, 9]. The N3-X aircraft is designed to reduce fuel/energy consumption by at least 60% relative to a conventional 2005 entry-into-service aircraft. Following the established performance characteristics of the selected baseline aircraft, mission level goals have been set for the N3-X aircraft in terms of payload and range requirements. The N3-X is therefore required to achieve a mission range of at least 7500 nmi, flying at Mach 0.84 with a full payload (payload mass equal to the aircraft maximum of 53,570 kg). In order to achieve the required efficiency improvements, the aircraft makes use of a number of novel technologies in both the airframe and the propulsion system. The aircraft propulsive power is provided by a distributed propulsion system consisting of an array of propulsor fans which ingest the boundary layer of the airframe. The propulsor array also ingests a portion of free-stream air in order to be capable of providing the required thrust. Electrical power for the propulsor fans is produced by a pair of turbogenerator type engines through a superconducting system, cooled by liquid hydrogen. The N3-X airframe is a blended wing body planform with main engines assumed to be embedded within the airframe (Figure 5). The embedded engine and propulsor array location provide noise shielding to achieve the required noise targets [25]. Fuel burn and emissions targets are achieved through utilisation of the boundary layer ingesting distributed propulsion system and blended wing body airframe with a high lift-to-drag ratio [4].

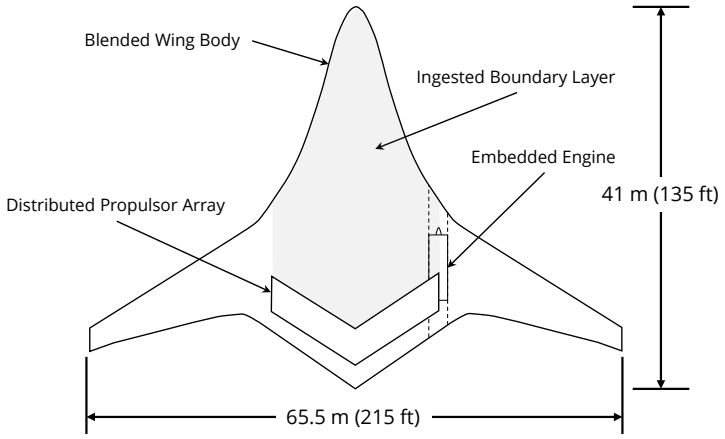

Figure 5: N3-X aircraft illustrative diagram

The case study made use of publicly available data and research on the aircraft: the aircraft and propulsor array configuration [9], and the boundary layer profiles at the centreline of the airframe [4]. The aircraft configuration provided the reference lengths (x, distance from the aircraft leading edge) necessary for estimation of the boundary layer thickness at locations other than the airframe centreline. As an initial estimate, the turbulent flat plate assumption was applied. To account for the discrepancy between the flat plate assumption and the actual aircraft configuration, the boundary layer thickness was scaled by a constant to match the available boundary layer profiles. The boundary layer profiles also provided an estimation of the local free-stream velocity at the edge of the boundary layer on the aircraft centreline. The velocity profile provided the local free-stream Mach number at the edge of the boundary layer from $x/c = 0.6$ to $x/c = 1.0$, where c is the centreline chord length. In the absence of a full CFD data analysis of the airframe, the velocity profile was extended to encompass the entire airframe. This included the assumption that the local free-stream velocity at the edge of the boundary layer would be equal at any axial distance x_0 from the aircraft nose. A more detailed estimate of airframe boundary layer and velocity distribution may be calculated using a more complete analysis of the airframe. However, the publicly available data was applied to demonstrate the analysis possible

Table 2: Propulsor array design parameters

ADP Altitude	30,000 ft
ADP Mach Number	0.84
Number of Propulsors	15
Fan Pressure Ratio	1.3
Fan Adiabatic Efficiency	0.9535
Inlet Stream AR	1.0
Net Propulsive Force	119 kN
Power Consumption	34.3 MW
SPC	288 W/N
Array Length	16.1 m

using the limited information that might be available at an early design stage. This is in keeping with the intended application of the method as a preliminary design tool.

In order to support the off-design simulations, it is assumed that the turbulent flat plate scaled to the N3-X configuration may used to estimate the boundary layer thickness at any of the simulated flight conditions. Difference in flow angle resulting from a change in aircraft incidence will be neglected, with the assumption that the fuselage acts as a 'flow straightener', and hence the inlet stream lies parallel to the fuselage surface once it reaches the interface point. Finally, it is assumed that the velocity profile for the airframe at design point may be scaled to the Mach number at the off-design flight condition.

5 Array Configuration

Previous research has simulated the array of the N3-X with a wide range of design parameters and configurations [8, 26]. The present research will consider a single configuration for the array with an aerodynamic design point (ADP) at Mach 0.84, 30,000 ft as defined by the original research on the N3-X (Table 2). The array consists of 15 propulsors with a design point pressure ratio of 1.3 and an adiabatic efficiency of 0.9535 [4]. The net propulsive force required at the design point is taken from previous research on the N3-X propulsion system as 119 kN [26]. The configuration used herein assumes that all the propulsive force is produced by the propulsor array. The array is sized such that each propulsor produces the same NPF at design point. In addition, it is assumed that each propulsor will have the same inlet stream aspect ratio ($\mathrm{AR} = w/h$).

The configuration of the aircraft means that each propulsor captures a different thickness of boundary layer and is subject to different flow conditions. The most efficient propulsor in terms of power consumption would be the centreline propulsor, as it ingests the thickest boundary layer and has a relatively low local velocity. As the propulsors advance along the fuselage span, the boundary layer thins and the local velocity increases, hence reducing the efficiency of the propulsors. The total pressure loss through the inlet of each propulsor is calculated following Seddon's method described in the previous section. Assuming that there is little variation in mass flow ratio across the length of the array, propulsors at the outer edges of the array will have a lower total pressure loss through the inlet than those near the centreline, due to a thinner boundary layer. However, the thinner boundary layer also means that those propulsors at the edges of the array have a higher power consumption than those nearer the centreline, as significantly more free-stream flow is ingested than boundary layer air [8]. The overall effect is a power consumption that is greater than it would be were the array to consist entirely of propulsors operating in the flow conditions at the centreline of the aircraft.

6 Off-design Performance

6.1 Individual Propulsors

A number of assumptions have been used in simulating the propulsor array of the N3-X at off-design. The primary assumption is that the propulsors have a variable area nozzle. This requirement was defined in previous research on the N3-X to ensure fan stability given the low fan pressure ratios being used for the propulsors [9]. Off-design mass flow matching is therefore required only between the fan and the mass flow of the inlet stream, following the procedure demonstrated in the previous section. The propulsors are assumed to operate on a peak efficiency running line and will have a constant non-dimensional mass flow for a fixed rotational speed. It should be noted that, due to the nature of boundary layer flow distortion, the actual running line of

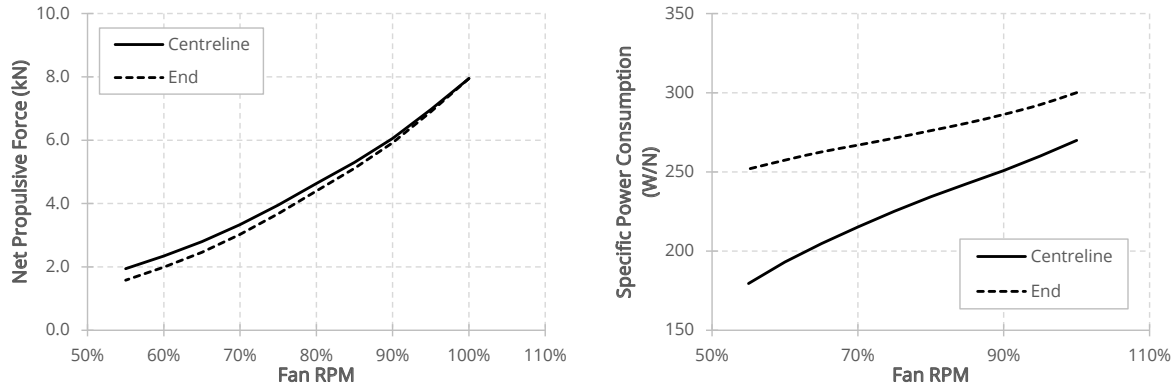

(a) Net propulsive force.

(b) Specific power consumption.

Figure 6: ADP performance of propulsors at the centreline and end of the propulsor array as a function of rotational speed.

the fan will depend on the flow and blade location. Certain segments of the fan may therefore operate closer or further towards surge than other segments [1, 22]. Different segments may also operate with different efficiencies and pressure ratios, assuming a fixed geometry fan.

Whilst the propulsors are sized to produce the same net propulsive force at design point, each propulsor will operate differently, due to differences in local flow characteristics and in non-dimensional mass flow. Therefore, each propulsor in the array will perform differently at off-design. To demonstrate this difference, the performance of two propulsors in the array, the centreline propulsor and the propulsor at the far end of the array, was simulated at the ADP flight conditions (Figure 6) and sea level static (Figure 7) for a range of fan rotational speeds (i.e. power settings).

Both propulsors are sized for the same NPF at design point, therefore, the reduction in net propulsive force as the fan rotational speed reduces is very similar (Figure 6a). However, the centreline fan produces slightly more net propulsive force than the end fan as the rotational speed reduces. Both fans operate on effectively the same running line (in terms of the relationship between rotational speed, efficiency, and pressure ratio) as they operate on the same scaled fan map. The difference in net propulsive force arises due to the difference in the proportion of drag ingested (i.e. boundary layer) between the two propulsors. Net thrust produced by the propulsors reduces for both propulsors as the rotational speed is reduced. The performance benefit due to ingesting the boundary layer is therefore more apparent as the rotational speed is reduced, as the centreline propulsor has a consistently lower momentum drag than a propulsor at the end of the array. In addition, as the propulsor at the centreline has a lower ratio of h/δ and a higher propulsive efficiency than a propulsor at the end of the array, the SPC of the centreline propulsor is consistently better than the end propulsor, despite producing similar thrust (Figure 6b). Reducing the rotational speed of the propulsor reduces its power consumption and increases its propulsive efficiency, hence SPC improves as the rotational speed is reduced.

At sea level static, the differences between the two propulsors reduce as the aircraft is static and the airframe boundary layer is effectively non-existent. In addition, the high mass flow ratio of sea level static operation means that the ratio of h/δ is high enough to make any ingested boundary layer negligible in comparison to the ingested free-stream flow. Location-specific differences therefore do not play a part in performance. As both propulsors are effectively operating with free-stream air (given the modelling assumptions), the total pressure loss through the inlet is similar. Therefore, the only difference in performance between propulsors results from a different size. All propulsors were sized to produce the same NPF at design point, however, this leads to a larger mass flow for propulsors at the outer edge of the array. As the performance benefits of the boundary layer do not contribute at static conditions, both propulsors have the same trend linking the decrease in rotational speed to a decrease in specific power consumption (Figure 7b). However, the difference between the two propulsors is apparent in their net propulsive force, comparable to net thrust when operating at sea level static conditions as D_{ingested} is zero (Figure 7a). The propulsor at the array end is larger than the centreline propulsor, as it is sized for a larger non-dimensional mass flow in order to produce the required net propulsive force at ADP. The propulsor at the array end is therefore able to produce more thrust than the centreline propulsor at sea level static conditions.

As the free-stream flow speed increases, the efficiency of the propulsors in the array diverges (Figure 8a). As with the change in rotational speed, the centreline propulsor is more efficient, due to a thicker ingested boundary layer and a lower local velocity. As the flight velocity reduces, the mass flow ratio of the propulsor

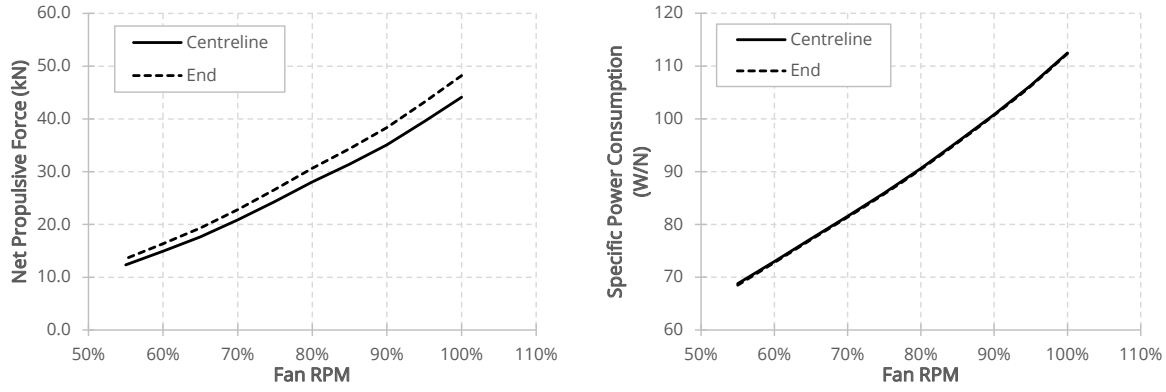

(a) Net propulsive force.

(b) Specific power consumption.

Figure 7: Sea level static performance of propulsors at the centreline and end of the propulsor array as a function of rotational speed.

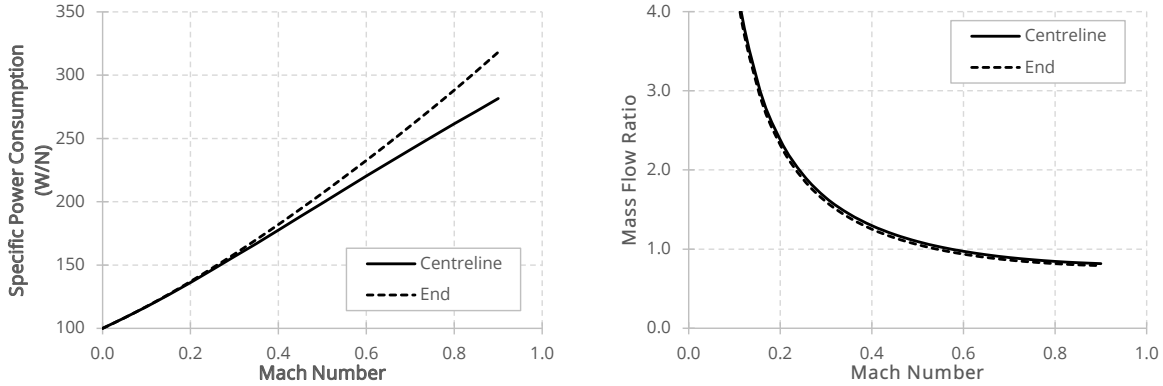

(a) Specific power consumption.

(b) Net propulsive force.

Figure 8: Performance of propulsors at the centreline and end of the propulsor array at 30,000ft as a function of Mach number

increases (Figure 8b). This is matched by a similar increase in the ratio h/δ , which tends the inlet flow characteristics, and hence performance, towards that of a free-stream propulsor (Figure 9). Flow characteristics as modelled are asymptotic to their free-stream values, however, for the simulated flight condition, average total pressure and velocity reach 99% of their free-stream value at a mass flow ratio of approximately 4, and 99.9% of their free-stream value at a mass flow ratio of approximately 50.

As the rotational speed of the fan is reduced, its mass flow demand also reduces. A low mass flow demand (below 1.0) implies an adverse pressure gradient, which leads to the risk of separation of the boundary before the inlet. The mass flow ratio is also linked to operating conditions (altitude and Mach number), with an increase in speed leading to a decrease in MFR. For the simulated configuration of the propulsor array, the propulsors at the outer edges operate at a lower MFR. However, the outer propulsors also operate with a thinner boundary layer, which may counterbalance the separation risk. The risk of boundary layer separation at low MFR must be addressed for BLI propulsion systems operating at high velocity and low power settings, such as flight idle during descent.

6.2 Whole Array

The performance of the array as a whole must account for each propulsor in the array, where the total net propulsive force and power demand is the sum of all the propulsors. At the aerodynamic design point, the lower efficiency of propulsors at the outer edges of the array reduces the overall efficiency of the array as a whole.

Initially, the performance of the propulsor array has been presented without considering the remainder of the propulsion system. The performance of the main engines and the power link between the main engines was therefore neglected and the propulsors in the array may run at a fixed rotational speed. This allows a

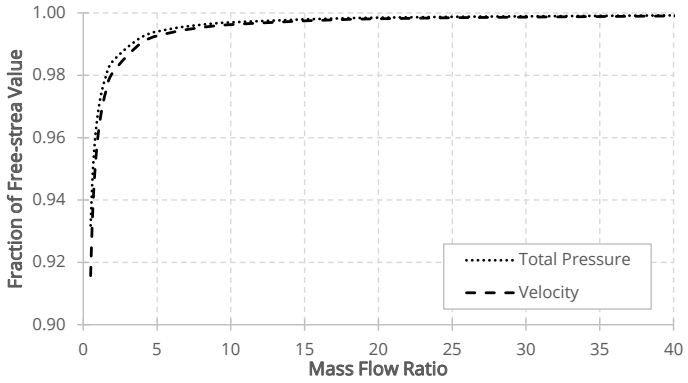

Figure 9: Mass flow-average total pressure and velocity of inlet stream as a function of mass flow ratio (85% chord)

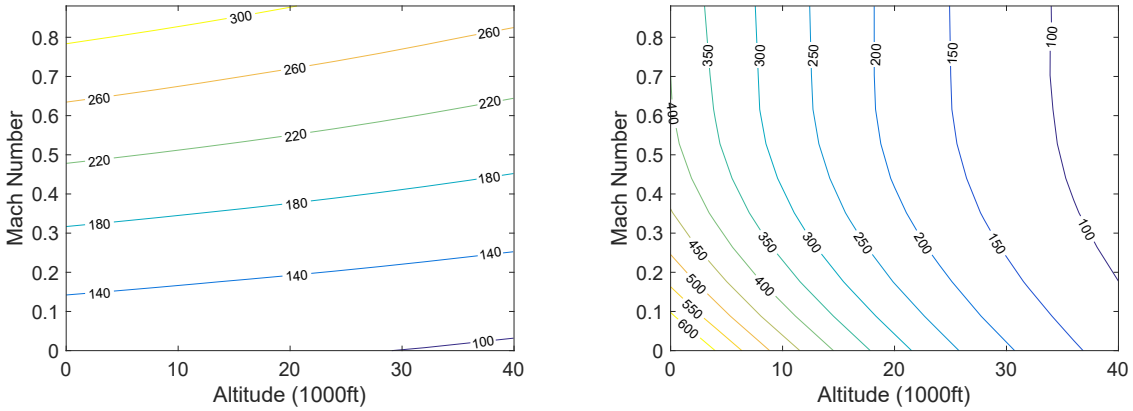

(a) Specific power consumption.

(b) Net propulsive force.

Figure 10: Propulsor array performance as a function of altitude and Mach number at 100% rotational speed

map to be produced that demonstrates the maximum potential net propulsive force of propulsor array at full power Figure 10b. As with a conventional system, more thrust can be produced at low speed, low altitude operating points. At low speed, the propulsion system is able to produce increasing amounts of thrust, as the momentum drag reduces due to the lower inlet velocity (despite a higher h/δ). At static conditions, h/δ tends to infinity, and hence the propulsor effectively operates in free-stream flow. This is matched by a lower specific power consumption at low altitude and low Mach numbers (Figure 7b). Although more thrust can be produced in these conditions, these conditions are also associated with a higher mass flow ratio (and hence higher h/δ), which slightly reduces efficiency. The overall specific power consumption nevertheless decreases overall for the system, due to the increase in thrust produced.

7 N3-X Propulsion System Case Study

The previous section predicted the performance of individual propulsors and the whole array for a range of power settings and flight conditions. However, the propulsion system of the N3-X consists of the propulsor array linked to a pair of turbogenerators through a superconducting electrical system. The performance of the array is therefore linked to the power available from the turbogenerators, whilst the performance of the turbogenerators is linked to the power demand from the propulsor array. Overall propulsion system efficiency must account for the performance of the gas turbines in combination with the propulsor array. As the energy to drive the turboelectric propulsion system is produced through combustion of conventional jet fuel, overall efficiency may be represented through specific fuel consumption. For the purposes of the N3-X propulsion system, specific fuel consumption will be represented with an effective specific fuel consumption (eSFC) term, the ratio between total fuel consumption of the gas turbines and the total net propulsive force (including any

Table 3: N3-X engine design parameters

ADP Altitude	30,000 ft
ADP Mach Number	0.84
Operating Pressure Ratio	64
Turbine Entry Temperature (K)	1811
Compressor Polytropic Efficiency	0.9325
Turbine Polytropic Efficiency	0.93
Power Turbine Polytropic Efficiency	0.924
Power	16.5 MW
Fuel Burn (kg/s)	0.657 kg/s

thrust produced by the gas turbines):

$$\mathrm{eSFC} = \frac{\dot{m}_{f,\mathrm{total}}}{NPF_{\mathrm{total}}} \tag{22}$$

An effective bypass ratio (eBPR) term will also be used, the ratio between the total bypass mass flow (i.e. the mass flow through the propulsor array), the the core mass flow (i.e. the mass flow passing through the gas turbine core and entering the combustor):

$$\mathrm{eBPR} = \frac{\dot{m}_{\mathrm{bypass}}}{\dot{m}_{\mathrm{core}}} \tag{23}$$

The design point power demand of the array establishes the required size of the turbogenerators. Each gas turbine produces half of the total power requirement, plus an additional amount to account for transmission efficiency of the superconducting electrical system (99.8% [4]). The turbogenerators are sized at design point for zero net thrust, however, some additional thrust may be produced at off-design. The split of thrust between the array and the turbogenerators will therefore vary. The turbogenerator design is based on previous research for the N3-X propulsion system. The engine is assumed to be a twin spool design with a free power turbine. The engine produces enough thrust at design point to counterbalance its drag. Compression is split between the low and high pressure compressors such that the enthalpy change over each compressor is the same [4]. A selection of key engine design parameters are shown in Table 3.

For the purposes of simulation, the performance of the propulsion system is calculated as one of two modes; an engine power matching mode and a propulsive force matching mode. For the power matching mode, an engine power setting is established (turbine entry temperature is used here), with propulsor array performance dictated by the available power produced by the main engines. In order to simplify the analysis, it is assumed that all propulsors in the array operate at the same rotational speed, with power distributed accordingly. Therefore, the rotational speed (and hence operating point) of the propulsors in the array is iterated until the power demand of the array matches the total power available through the superconducting electrical system (Figure 11a). An alternate simulation methodology would be to assume that each propulsor is provided with the same power, and iterate the rotational speed of each propulsor independently to determine their operating point. The propulsive force matching mode is used to calculate the propulsion system performance where the net propulsive force requirement is know, such as the thrust equal to drag requirement for steady level flight during cruise. At off-design, both the array and the gas turbines may produce thrust. The split between thrust produced by the main engines and the propulsor array is unknown. Therefore, engine power is instead iterated until the total propulsive force produced by the combined system equals the required value (Figure 11b).

As an additional limitation to the performance of the N3-X's propulsion system, it is also feasible to assume that the rotational speed of the motors driving the fans will not exceed 100% of their maximum value. If the power supplied to the array would result in a rotational speed above 100%, the array performance must be capped. Any excess power is assumed to either charge battery storage or power internal systems. Alternatively, the propulsion system may be run at a lower power setting.

A comparison of the system performance to previous research is challenging, as the present research includes the spanwise variation in flow characteristics over the array length, an aspect not considered in previous simulations. In addition, the difference in force accounting and boundary layer and airframe flow characterisation at off-design will lead to differences in the final results. Nevertheless, a general comparison may be used to estimate whether performance matches expectations and requirements from previous research. Previous research on the N3-X has predicted the propulsion system's performance at a selection of key operating points; the aerodynamic design point, rolling take-off (RTO) at sea level and Mach 0.25, and sea level static (SLS). In addition, a cruise point at 40000 feet and Mach 0.84 was simulated [26]. The control

(a) Engine power matching **(b)** Propulsive force matching

Figure 11: Simulation procedure for N3-X propulsion system operating modes

Table 4: N3-X engine operating points as defined in Reference [26].

	ADP	Cruise	RTO	SLS
Altitude (ft)	30000	40000	0	0
Mach Number	0.84	0.84	0.25	0
Engine TET (K)	1811	1728	1895	1922
Power Consumption (MW)	32.9	20.0	58.2	60.5
Specific Power Consumption (W/N)	276.5	265.0	152.5	103.7
eSFC (mg/Ns)	11.04	10.50	6.69	4.53
eBPR	32.5	32.4	32.7	32.3
NPF (kN)	119.0	75.6	389.2	599.4
Thrust Split	100%	100%	98.0%	97.4%
Propulsor RPM	100%	100%	91%	93%

parameter for each of the simulated operating points was the engine turbine entry temperature (TET), i.e. the array was simulated using the engine power matching operating mode. The resulting performance for each operating was compared against previous simulations for the N3-X performed by Felder et al. The net propulsive force produced at take-off corresponds with the 552.3 kN value quoted in the referenced research [26]. There is a greater deviation in net propulsive force at RTO, which is 368.9 kN in comparison to the 301.8 kN value obtained in the previous research. This value is nevertheless of the same order as previous simulations for the N3-X propulsion system. The cruise net propulsive force agrees with the 74 kN value predicted by previous research [26]. The present research accounts for the change in flow characteristics along the length of the array, this leads to a lower array efficiency which increases SFC by approximately 6% at cruise in comparison by previous research.

Given the assumptions made, the main engines were found to be a limiting factor on the performance of the propulsor array at the RTO and SLS operating points. The maximum power available from the power turbines at the two operating points is lower than that required to operate the propulsors at 100% rotational speed. The propulsors must therefore run at a lower rotational speed (91% at RTO and 93% at SLS). The total net propulsive force is therefore lower than would be possible were the propulsor array to be run at full power. The net propulsive force produced by the propulsor array is nevertheless high enough to exceed the take-off thrust requirements established by previous research.

The discrepancy between the propulsor array and main engine performance means that the propulsor array will rarely operate at a point where maximum power demand exactly matches the maximum available power from the free power turbines (Figure 12). At lower altitudes the maximum power demanded by the array at 100% rotational speed exceeds the available power. In contrast, at higher altitudes the available power at the ADP power setting exceeds the maximum power demand of the propulsor array (assuming a maximum propulsor RPM of 100%). The power deficit at low altitude is significantly greater than the power excess at high altitudes. The higher engine power settings of take-off and climb will reduce the power deficit, but the power demand from the propulsor array is nevertheless greater than the power the main engines are able to supply.

After accounting for the power deficit at low altitudes, a map of the overall propulsion system performance may be created (Figure 13). In contrast to the potential net propulsive force available from the propulsor

array, the actual net propulsive force is lower, due to the power deficit. However, a measure of additional propulsive force is produced by the main engines that slightly increases the propulsion system's total net propulsive force.

Finally, the assumption that the fan motors cannot 'overspeed', i.e. will not operate above the maximum rotational speed, may be applied. This reduces the available thrust at higher altitudes where there is a power excess (Figure 14). The main engines may then be operated at a lower power setting to match the cap on the propulsor array performance and hence the slightly lower power demand Figure 14. Alternatively, the excess power at high altitudes shown in Figure 12 may be used for other aircraft subsystems or battery charging. The point where the array performance is capped by the maximum rotational speed limit is clearly visible as a kink in the net propulsive force and specific fuel consumption trends with altitude and Mach number. Similarly, the point where array performance is capped by the maximum available power is visible where the net propulsive force trend begins to diverge away from the maximum net propulsive force predicted in Figure 10b.

8 Conclusions

Research suggests that boundary layer ingesting propulsion systems may provide benefits to an aircraft's performance and lead to reductions in energy consumption. As research on BLI aircraft progresses, it becomes important to develop methods that may be used to model such propulsion systems not only at design point, but also over the full flight envelope. This research has presented a methodology intended for use as a preliminary design tool that may be used to explore the design space and identify design challenges or potential optimum configurations. The research has presented a work flow and process for modelling a boundary layer ingesting propulsion system at off-design. The method expands on previous research developing methods for the sizing and assessment of BLI propulsion systems at design point. Following on from previous research [8], the average flow characteristics of the incoming streamtube are a function of the streamtube size and the ratio of inlet stream height to boundary layer thickness, h/δ. Off-design mass flow demand of the propulsor or propulsion system is used to determine the inlet stream size and inlet flow characteristics. The reliance of downstream propulsor performance on the size of the inlet stream necessitates a mass flow matching procedure to determine the mass flow ratio of the incoming streamtube. This mass flow matching procedure adds an additional step to the component matching to determine the operating point of gas turbine components (e.g. compressor or turbine maps).

The tool has been used to model the propulsion system of a novel aircraft, the N3-X, as a case study. In this configuration, the fan rotational speed was used as a handle for determining off-design performance. Rotational speed is used to determine the propulsor operating point and hence mass flow demand. The N3-X's distributed propulsor array is linked to a pair of turbogenerators which provide power through a superconducting electrical system. Propulsors at different locations along the array were found to perform differently at off-design, due differences in the incoming flow characteristics and propulsor size. At design point flight conditions (30,000ft, Mach 0.84), propulsors on the aircraft centreline were found to be more efficient than those at the outer edges of the array, due to a thicker boundary layer and slower local flow. However, simulations found that at sea level static ratio (i.e. high mass flow ratio and thing to non-existent boundary layer), the difference in efficiency was negligible. Instead, the only difference in performance was a higher net propulsive force resulting from differences in propulsor size.

With high mass flow ratio operation, the ratio of h/δ is high, and hence average inlet flow characteristics are effectively equal to the free-stream flow characteristics. in addition, for slow or static aircraft, the boundary layer thickness is negligible. The primary difference in performance between propulsors at high mass flow ratio would therefore also be be due to a differences in propulsor size rather than different flow characteristics.

The propulsion system's performance was compared to the performance predicted by previous research. Propulsive force at sea-level static and rolling take-off produced by the array was found to be higher than that previously predicted as the propulsors are effectively operating with free-stream flow characteristics at RTO and SLS. This leads to an increase in thrust produced by the propulsor. However, this also leads to a high power demand at the maximum fan rotational speed which cannot be matched by the power available from the main engines as simulated.

Given the assumption used for modelling the N3-X propulsion system, there is only a narrow operating region where the power supply and demand of the propulsor array and main engines coincides. For high altitudes, the power available from the main engines at the ADP power settings exceeds the power required by the propulsors in the array at their maximum rotational speed. In contrast, for lower altitudes, the power required from the propulsors at maximum rotational speed exceeds the power available from the main engines at their ADP power setting.

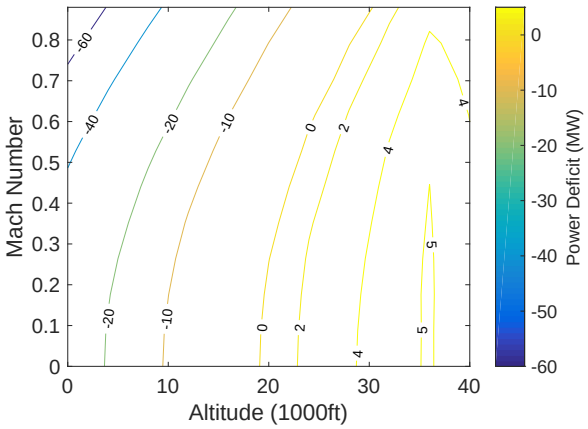

Figure 12: Power deficit between propulsor array and main engines at ADP power setting as a function of altitude and Mach number

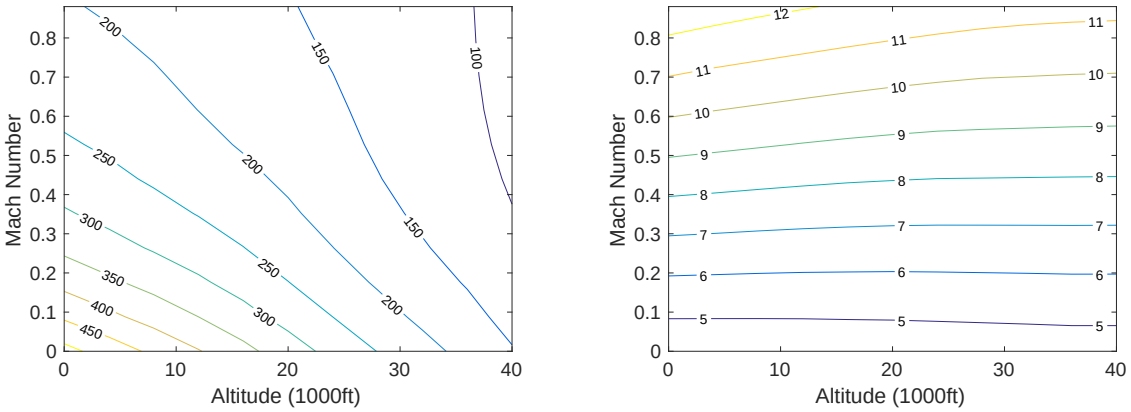

(a) Net propulsive force (kN) **(b)** Specific fuel consumption (mg/Ns)

Figure 13: Propulsion system performance as a function of altitude and Mach number (ADP engine power setting: TET = 1811 K)

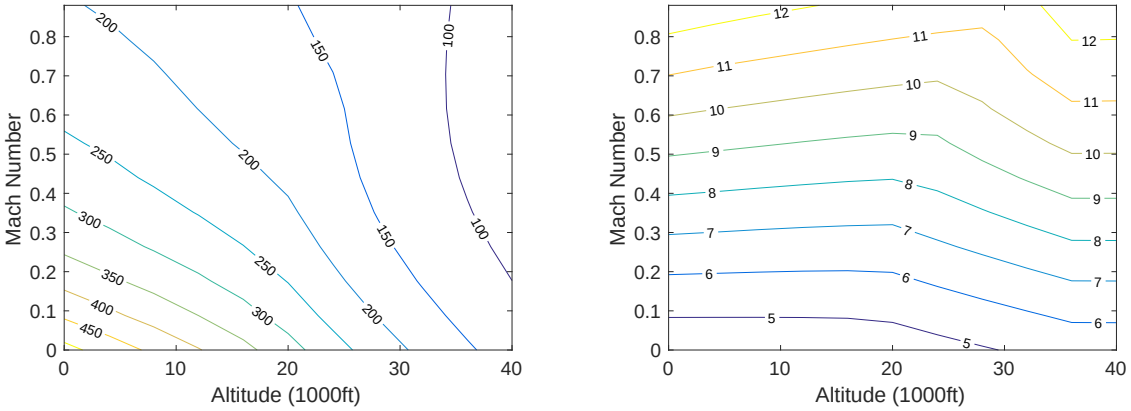

(a) Net propulsive force (kN) **(b)** Specific fuel consumption (mg/Ns)

Figure 14: Propulsion system performance as a function of altitude and Mach number (Array capped at 100% design rotational speed, ADP engine power setting until propulsor array speed cap)

9 Further Work

The research presented herein has considered the performance of a single configuration of the N3-X propulsion system. However, the configuration of the propulsion system presents a large number of degrees of freedom for the design that may lead to a more efficient design. Previous research on the N3-X propulsion system has shown that a more efficient system may be found if the source of thrust is split between the propulsor array and main engines [7]. It is therefore necessary to simulate alternative configurations in order to compare their performance and select the most efficient designs.

The method presented in this research enables the rapid analysis of novel BLI configurations at a preliminary design stage. It can therefore be used to identify the most efficient configurations as development progresses. However, modelling procedures with a higher level of fidelity will be required as designs advance to address the assumptions that are necessary for simulating conceptual designs.

Acknowledgements

The authors would like to extend their gratitude to NASA for making this work possible under grant number NNX13AI78G. Many thanks go also to staff at Cranfield University for their advice and assistance.

References

[1] A P Plas, M A Sargeant, V Madani, D Crichton, E M Greitzer, T P Hynes, and C a Hall. Performance of a Boundary Layer Ingesting (BLI) Propulsion System. In *45th AIAA Aerospace Sciences Meeting and Exhibit, 8 - 11 January 2007, Reno, NV, USA*, number AIAA 2007-450, 2007. doi: 10.2514/6.2007-450.

[2] Leroy H. Smith. Wake ingestion propulsion benefit. *Journal of Propulsion and Power*, 9(1):74–82, 1993. ISSN 0748-4658. doi: 10.2514/3.11487.

[3] Larry W Hardin, Gregory Tillman, Om P Sharma, Jeffrey Berton, and David J Arend. Aircraft System Study of Boundary Layer Ingesting Propulsion. In *48th AIAA/ASME/SAE/ASEE Joint Propulsion Conference and Exhibit, Atlanta, GA, USA*, number AIAA 2012-3993, 2012. doi: 10.2514/6.2012-3993.

[4] James Felder, Gerald Brown, Hyun Kim, and Julio Chu. Turboelectric Distributed Propulsion in a Hybrid Wing Body Aircraft. In *20th International Society for Airbreathing Engines, Gothenburg, Sweden*, number ISABE-2011-1340, 2011.

[5] Mark Drela. Power balance in aerodynamic flows. *AIAA journal*, 47(7):1761–1771, 2009. doi: 10.2514/1.42409.

[6] Aurélien Arntz, Olivier Atinault, and Alain Merlen. Exergy-Based Formulation for Aircraft Aeropropulsive Performance Assessment: Theoretical Development. *AIAA Journal*, 53(6):1627–1639, 2014. doi: 10.2514/1.J053467.

[7] Esteban A Valencia, Devaiah Nalianda, Panagiotis Laskaridis, and Riti Singh. Methodology to assess the performance of an aircraft concept with distributed propulsion and boundary layer ingestion using a parametric approach. *Proceedings of the Institution of Mechanical Engineers, Part G: Journal of Aerospace Engineering*, 229(4):682–693, 2015. doi: 10.1177/0954410014539291.

[8] Chana Goldberg, Devaiah Nalianda, Pericles Pilidis, David MacManus, and James Felder. Installed performance assessment of a boundary layer ingesting distributed propulsion system at design point. In *52nd AIAA/SAE/ASEE Joint Propulsion Conference*, number AIAA 2016-4800, 2016.

[9] James L Felder, Hyun Dae Kim, and Gerald V Brown. Turboelectric distributed propulsion engine cycle analysis for hybrid wing body aircraft. In *47th AIAA Aerospace Sciences Meeting, Orlando, FL, USA*, number AIAA 2009-1132, 2009. doi: 10.2514/6.2009-1132.

[10] AGARD. Guide to In-Flight Thrust Measurement of Turbojets and Fan Engines. *AGARD 237*, 1979.

[11] AP Plas. Performance of a boundary layer ingesting (BLI) propulsion system. Master's thesis, 2006.

[12] Darrell Williams. Application of boundary layer theory to BLI simulation [Personal Communications], 2015.

[13] J D Anderson. *Fundamentals of Aerodynamics*. McGraw-Hill Education, 1991. ISBN 0072373350. doi: 10.1371/journal.pcbi.1000716.

[14] B. S. Stratford and G. S. Beavers. The Calculation of the Compressible Turbulent Boundary Layer in an Arbitrary Pressure Gradient-A Correlation of certain previous Methods. Technical Report ARC-3207, Aeronautical Research Council, 1961.

[15] Hermann Schlichting. Boundary layer theory. part 2 - turbulent flows. Technical Report NACA-TM-1218, Zentrale fuer Wissenschaftliches Berichtswesen, Berlin, Germany, 1949.

[16] Herrmann Schlichting and Klaus Gersten. *Boundary-layer theory*. Springer, 2000. ISBN 3540662707.

[17] Jonathan C Gladin, Brian K Kestner, Jeff S Schutte, and Dimitri N Mavris. Engine Design Strategy for Boundary Layer Ingesting Propulsion Systems With Multiple Non-Symmetric Engine Inlet Conditions. In *ASME Turbo Expo 2013: Turbine Technical Conference and Exposition, San Antonio, TX, USA*, number GT2013-95905, 2013. doi: 10.1115/GT2013-95905.

[18] Bobby L Berrier and Brian G Allan. Experimental and Computational Evaluation of Flush-Mounted, S-Duct Inlets. In *42nd AIAA Aerospace Sciences Meeting and Exhibit, Reno, NV, USA*, number AIAA 2004-764, 2004. doi: doi:10.2514/6.2004-764.

[19] Susan Althoff Gorton, Lewis R Owens, Luther N Jenkins, Brian G Allan, and Ernest P Schuster. Active flow control on a boundary-layer-ingesting inlet. In *42nd AIAA Aerospace Sciences Meeting and Exhibit, Reno, NV, USA*, number AIAA 2004-1203, 2004. doi: 10.2514/6.2004-1203.

[20] J Seddon. *Boundary-layer interaction effects in intakes with particular reference to those designed for dual subsonic and supersonic performance*. Aeronautical Research Council, 1970.

[21] Panagiotis Laskaridis. Assessment of distributed propulsion systems used with different aircraft configurations. In *51st AIAA/SAE/ASEE Joint Propulsion Conference*, pages AIAA 2015–4029, 2015.

[22] Chengyuan Liu, Daniel Ihiabe, Panagiotis Laskaridis, and Riti Singh. A preliminary method to estimate impacts of inlet flow distortion on boundary layer ingesting propulsion system design point performance. *Proceedings of the Institution of Mechanical Engineers, Part G: Journal of Aerospace Engineering*, 228 (9):1528–1539, 2014. doi: 10.1177/0954410013496750.

[23] Arne Seitz and Corin Gologan. Parametric design studies for propulsive fuselage aircraft concepts. *CEAS Aeronautical Journal*, 6(1):69–82, 2015. doi: 10.1007/s13272-014-0130-3.

[24] Andrew Rolt and John Whurr. Optimizing Propulsive Efficiency in Aircraft with Boundary Layer Ingesting Distributed Propulsion. In *22nd International Symposium on Air Breathing Engines, 25 - 30 October 2015, Phoenix, AZ, USA*, number ISABE-2015-20201, 2015.

[25] J Berton and W Haller. A noise and Emissions Assessment of the N3-X Transport. In *52nd Aerospace Sciences Meeting, National Harbor, MD, USA*, number AIAA 2014-0594, 2014. doi: 10.2514/6.2014-0594.

[26] James L Felder, Hyun Dae Kim, and Gerald V Brown. An Examination of the Effect of Boundary Layer Ingestion on Turboelectric Distributed Propulsion Systems. In *49th AIAA Aerospace Sciences Meeting, Orlando, FL, USA*, number AIAA 2011-300, 2011. doi: 10.2514/6.2011-300.